

Accepted Manuscript

Title: Swelling and shrinking behaviour of photoresponsive phosphonium-based ionogel microstructures

Author: Monika Czugala Claire O'Connell Candice Blin Peer Fischer Kevin J. Fraser Fernando Benito-Lopez Dermot Diamond



PII: S0925-4005(13)01553-0
DOI: <http://dx.doi.org/doi:10.1016/j.snb.2013.12.072>
Reference: SNB 16370

To appear in: *Sensors and Actuators B*

Received date: 18-10-2013
Revised date: 9-12-2013
Accepted date: 18-12-2013

Please cite this article as: M. Czugala, C. O'Connell, C. Blin, P. Fischer, K.J. Fraser, F. Benito-Lopez, D. Diamond, Swelling and shrinking behaviour of photoresponsive phosphonium-based ionogel microstructures, *Sensors and Actuators B: Chemical* (2013), <http://dx.doi.org/10.1016/j.snb.2013.12.072>

This is a PDF file of an unedited manuscript that has been accepted for publication. As a service to our customers we are providing this early version of the manuscript. The manuscript will undergo copyediting, typesetting, and review of the resulting proof before it is published in its final form. Please note that during the production process errors may be discovered which could affect the content, and all legal disclaimers that apply to the journal pertain.

Swelling and shrinking behaviour of photoresponsive phosphonium-based ionogel microstructures

Monika Czugala,^a Claire O'Connell,^a Candice Blin,^b Peer Fischer,^c Kevin J. Fraser,^a
Fernando Benito-Lopez,^{a,d*} and Dermot Diamond^a

^a CLARITY: Centre for Sensor Web Technologies, National Centre for Sensor
Research, Dublin City University, Dublin 9, IRELAND

^b Fraunhofer Institute of Physical Measurement Techniques IPM, 79110 Freiburg,
GERMANY

^c Max Planck Institute for Intelligent Systems, Heisenbergstr. 3, 70569
Stuttgart, GERMANY

^d CIC microGUNE, Arrasate-Mondragón, SPAIN

Corresponding Author

*Phone: +34 943710237. Fax: +34 943739805. E-mails: fernando.lopez@dcu.ie and
fbenito@cicmicrogune.es.

Keywords

Stimuli responsive, photo-responsive, microstructures, photo-patterning, ionogel,
ionic liquid.

Abstract

Photoresponsive *N*-isopropylacrylamide ionogel microstructures are presented in this study. These ionogels are synthesised using phosphonium based room temperature ionic liquids, together with the photochromic compound benzospiropyran. The microstructures can be actuated using light irradiation, facilitating non-contact and non-invasive operation. For the first time, the characterisation of the swelling and shrinking behaviour of several photopatterned ionogel microstructures is presented and the influence of surface-area-to-volume ratio on the swelling kinetics is evaluated. It was found that the swelling and shrinking behaviour of the ionogels is strongly dependent on the nature of the ionic liquid. In particular, the [P_{6,6,6,14}][NTf₂] ionogel exhibits the greatest degree of swelling, reaching up to 180 % of its initial size, and the fastest shrinkage rate ($k_{sh} = 29 \pm 4 \times 10^{-2} \text{ s}^{-1}$).

1. Introduction

Stimuli responsive materials, such as gels, have recently attracted widespread attention due to their highly attractive properties, including mechanical, optical, surface and permeability characteristics, which can be tuned in response to an externally applied stimulus.¹ The changes can be induced with different stimuli depending on the switchable functional group attached to the gel network, *e.g.* magnetic,² thermal,³ light,⁴ pH⁵ or electrochemical stimuli.⁶

In particular, *N*-isopropylacrylamide (NIPAAm) has been widely studied as a base material for stimuli responsive gels, due to the high degree of swelling at low temperatures, large volume change upon crossing the volume transition temperature,

in this case, the lower critical solution temperature (LCST).⁷ One of the most attractive approaches to polymer actuation is light irradiation,⁸ as it allows non-contact and non-invasive operation. This can be achieved by functionalising poly(*N*-isopropylacrylamide) gels p(NIPAAm) with spirobenzopyran chromophores (SP), which are capable of interconversion between two thermodynamically stable states under light external stimulus.

Functionalising the p(NIPAAm) gels with SP produces hybrid materials (which we shall henceforth refer to as p(SPNIIPAAm)), consisting of two stimuli responsive entities:

1. The thermoresponsive p(NIPAAm) gel which swells below its lower critical solution temperature (LCST);⁹
2. The photoresponsive spiropyran molecule, SP, that is able to open to the charged MC under UV-irradiation and revert to the uncharged SP isomer under white light irradiation.

Normally the p(SPNIIPAAm) gel is soaked in an aqueous solution of HCl (typically pH 3) to induce spontaneous isomerisation to the protonated merocyanine (MC-H⁺) form, which has a yellow colour due to absorption in the visible spectrum by MC-H⁺ (λ_{max} usually in the range 420-440 nm). The protons diffusing into the gel are accompanied by counter ions and water, causing the gel to swell and adopt a more hydrophilic conformation. Upon irradiation with white light, the MC-H⁺ reverts to the uncharged, colourless SP form, which triggers dehydration and shrinkage of the gel.¹⁰

The effects of ring-opening rates of spirobenzopyran derivatives on light-induced volume change behaviour of gels have been reported previously.⁸ Several

spirobenzopyran derivatives, having different ring-opening rates, were introduced into p(NIPAAm) hydrogels and the effects on volume changes of these gels were evaluated by Satoh *et al.*¹¹ It was found that the rates of the spontaneous re-swelling of the p(SPNIpAAm) gels from light-induced shrunken state increased with increasing ring-opening rates of the spirobenzopyran molecules in the gels. Furthermore, rod-like and sheet-like p(SPNIpAAm) gels were investigated as potential light-responsive soft actuators and micro-conveyors, respectively. Sugiura *et al.*,¹⁰ for instance, presented the independent control of multiple p(SPNIpAAm) microvalves, which were fabricated by *in situ* photo-polymerisation at desired positions within microchannels. Blue light irradiation of the microvalves induced shrinkage of the gels and caused the microvalves to open after 18 - 30 s irradiation.

Traditionally, organic solvents such as 1-butanol,¹⁰ dimethyl sulfoxide,¹² 1,4-dioxane–water¹¹ and tetrahydrofuran/water¹³ mixture solutions have been used for the preparation of p(SPNIpAAm) gels. A new approach is to incorporate ionic liquids (ILs) as solvents within polymer matrices to produce a new class of hybrid materials known as ionogels. Defined as “a solid interconnected network spreading throughout a liquid phase”, the ionogel combines the physical properties of both the polymer gel and the physically entrapped IL.¹⁴ It was reported that certain ionogels exhibit enhanced water uptake/release behaviour, and improved mechanical and viscoelastic properties compared to the equivalent hydrogel.¹⁵ We have recently published several papers on phosphonium-based ILs, and their use in ionogels.^{16, 17, 18}

In this paper, we report the synthesis of photoresponsive poly(*N*-isopropylacrylamide) ionogels functionalised with spiropyran chromophores, and examine their ability to be photopatterned into complex microstructures using a

simple and inexpensive photolithography set-up capable of generating 3D arrays of microstructures. In the case of volume change photoresponsive materials, their performance is determined by the swelling and shrinking behaviour, and therefore it is one of the basic properties that needs to be considered if it is to form the basis of a useful polymer actuator.⁸ Due to the large surface-area-to-volume ratio of the photopatterned microstructures compared to bulk macro scaled gel structures, the rates of water diffusion into and out of the gel are highly accelerated. The polymer anchoring restricts movement of the gel along the surface of the substrate, and therefore swelling at the ionogel-glass substrate interface is inhibited, leading to highly anisotropic gel expansion primarily in the direction away from the surface.¹⁹ Height changes measurements of the ionogel microstructures were used to investigate their swelling and shrinking behaviour. The light-induced volume change of the ionogel microstructures was fully characterised to examine the dependence of their swelling and shrinking behaviour on the dimensions of the photopatterned microstructures, and on the particular phosphonium based ionic liquid used. We believe that such three-dimensional (3D) microstructures, fabricated using this approach, have a wide range of potential applications in micro-electromechanical systems (MEMS), sensors/actuators, optical devices and micro-fluidics.

2. Experimental

2.1. Ionogel Materials

N-isopropylacrylamide, *N,N'*-methylene-bis(acrylamide) (MBAAm), 2,2-5 dimethoxy-2-phenyl acetophenone (DMPA) were used for ionogel preparation as

purchased from Sigma-Aldrich[®], Ireland. 1', 3', 3'-Trimethyl-6-hydroxyspiro(2H-1-benzopyran- 2, 2'-indoline) (Acros Organics, Geel, Belgium), 3-(Trimethoxysilyl) propyl methacrylate was purchased from Sigma Aldrich[®], Ireland. Trihexyltetradecyl-phosphonium dicyanoamide [P_{6,6,6,14}][dca], trihexyltetradecyl-phosphonium bis(trifluoromethanesulfonyl)-amide [P_{6,6,6,14}][NTf₂], trihexyltetradecyl-phosphonium chloride [P_{6,6,6,14}][Cl] were obtained as compliments of Cytec[®] Industries, Ontario, Canada, Figure 1a. Further purification was carried out as follows: 10mL of IL decolourised by redissolution in 30 mL of acetone followed by treatment with activated charcoal (Darco-G60, Aldrich) at 40 °C overnight. Carbon was removed by filtration through alumina (acidic, Brockmann I, Aldrich) and the solvent removed under vacuum at 60 °C for 24 h at 0.1 Torr.

170 µm thick glass slides were purchased from Sigma Aldrich[®], Ireland. High power UV-365 nm light emitting diode was obtained from Electrolyte Corporation, USA.

2.2. Preparation of the ionogel prepolymer mixture

All the ionogels contain *N*-isopropylacrylamide (Figure 1b, y), *N,N'*-methylene-bis(acrylamide) (Figure 1b, z) and 1', 3', 3'-Trimethyl-6-acrylate(2H-1-benzopyran- 2,2'-indoline) (Figure 1b, x) in the ratio of 100: 5: 1, respectively. The acrylated benzospiropyran was synthesised as described elsewhere.²⁰ A liquid prepolymer mixture was prepared by dissolving the NIPAAm monomer (7.0 mmol), the MBAAm (0.07 mmol), acrylated spirobenzopyran monomer (0.75 mmol), and the

photo-initiator DMPA (0.35 mmol) into the ionic liquid. Three types of phosphonium based ionic liquids were tested [P_{6,6,6,14}][dca], [P_{6,6,6,14}][Cl] and [P_{6,6,6,14}][NTf₂]. In order to dissolve the monomers, the solution was heated to 40 °C using an ultrasonic bath (Bennett Scientific Ltd.) for 15 min.

FIGURE 1

Figure 1. Chemical structure of A) the phosphonium cation and the anions selected for the ionogel formulation - dicyanoamide [dca]⁻ (left), chloride [Cl]⁻ (middle) and bis(trifluoro-methanesulfonyl)-imide [NTf₂]⁻ (right); B) the crosslinked pNIPAAm ionogel functionalised with acrylated spiropyran. C) Schematic illustration of the surface-attached polymer network reversibly swelling/contracting in one dimension away from the substrate due to movement of protons (H⁺), counter ions (A⁻) and water in/out of the gel.

This approach allowed the fabrication of ionogel microstructures of various dimensions and geometries simultaneously from the mask (Figure S2), from large (radius 500 μm) to small (radius 200 μm) discs, lines (length 1100 μm, width 500 μm) and rings (1500 μm external diameter by 1100 μm inner diameter), see supportive information Figure S3.

2.3. Surface functionalisation

To facilitate homogeneous covalent bonding between the ionogel and the glass slide, the surface of the slide was chemically functionalised using method published previously by Hou *et al.*²¹ After washing with acetone, methanol, ethanol (all from

Brenntag UK & Ireland) and DI water, bare glass slides were incubated with 1 M sodium hydroxide (NaOH) (Sigma Aldrich, Ireland) for 10 min, flushed with DI water, and then purged by vacuum. A degassed 2:3:5 (v/v/v) mixture of 3-(trimethoxysilyl)-propyl methacrylate (MPTMS) (Sigma Aldrich, Ireland), glacial acetic acid (Merck KgaA, Germany), and DI water was then placed on the glass slides for silane monolayer formation. After 30 min incubation, the glass slides were rinsed for 10 min with methanol and DI water and dried under vacuum.

Contact angle measurements were performed using a FTA 200[®] dynamic contact angle analyser, using deionised water as the probing liquid. All measurements were undertaken under ambient humidity and temperature conditions. The values quoted are the averages of four individual measurements.

2.4. Characterisation of the photo-responsive phosphonium-based ionogels

The *in-house* designed and built optical set-up and the protocol used for the photopolymerisation of photo-responsive phosphonium-based ionogel micropattern is presented in the Supporting Information, Figure S1. The volume phase-transition behaviour of the microstructures was investigated using an Aigo Digital Microscope GE -5 and VHX-2000 3D Keyence Digital Microscope. The percent variation in ionogel microstructure height, %*H*, is defined as

$$\%H = (H_t - H_0) / H_0 \times 100 \quad (1)$$

where H_t is the height of the ionogel microstructure at time t and H_0 is the height

before immersion in 1 mM HCl solution. The kinetics of swelling was investigated by placing the [P_{6,6,6,14}][NTf₂], [P_{6,6,6,14}][dca] and [P_{6,6,6,14}][Cl] ionogel samples in a dark environment in 1 mM HCl aqueous solution, and taking digital images every 20 min for 140 min. A single exponential model (Eqn. 1)²² was used to estimate the swelling rate constants:

$$\%H = a \times (1 - e^{-k_{sw}t}) + b \quad (2)$$

where $\%H$ is the percentage swelling, a is a scaling factor, k_{sw} is the first order rate constant (s^{-1}), b is the baseline offset and t is time (s).

The kinetics of the gel shrinking was evaluated by irradiating the disc-shaped ionogels with the white light coming from the Aigo Digital Microscope GE -5 for 30 min. Pictures were taken with the same microscope after 1, 3, 5, 10, 15, 20, 25 and 30 min of exposure. The shrinking rate constants were estimated using the following exponential decay model (Eqn. 2):

$$\%H = a \times e^{-k_{sh}t} + b \quad (3)$$

where $\%H$ is the percentage swelling (calculated in the same manner as for equation (1) above), a is a scaling factor, k_{sh} is the first order rate constant (s^{-1}), b is the baseline offset and t is time (s).

All measurements were carried out at 21 °C. In order to measure the height change of the microstructures while swelling and shrinking, the glass slide with photopatterned ionogels was placed perpendicularly to the lens. In order to get a sharp focus, the glass slides were cut as close to the microstructures as possible (*ca.* 500

µm).

SEM studies were performed using a Carl Zeiss EVOLS 15 Scanning Electron Microscopy system at an accelerating voltage of 26.11 kV. Gold sputtering of all ionogels was performed on a Polaron® SC7640 Auto/Manual High Resolution Sputter Coater. All ionogels were coated under the following conditions: voltage 1.5 kV, 15 mA for 2 minutes at a coating rate of 5 nm min⁻¹. The 10 nm gold coating proved capable of maintaining a hydrated ionogel for microscopy imaging.

3. Results and discussion

3.1. Substrate surface modification

In initial experiments, the glass surfaces were not modified to assist adhesion of the ionogel. Although the ionogel patterns were properly formed using this approach, the polymer array elements easily delaminated upon hydration due to swelling of the ionogel matrices and detachment of the microstructures from the slide surface. In order to prevent this delamination of the swollen ionogels from the substrate, the slide surfaces were treated with MPTMS, generating a monolayer vinylised surface. The water contact angle values before and after each step of the treatment are shown in Table S1, Supporting Information. The results demonstrate that the method provides a more hydrophobic surface than the bare glass. The final contact angle of the treated glass substrates was $72 \pm 4^\circ$ ($n = 4$). The ionogel was then photo-polymerised on the vinyl surface generating covalent bonds between the functionalised slide surface and the microstructures. By anchoring the ionogel network to the glass substrate in this

manner, the mechanical stability of the ionogels microstructures is greatly increased.¹⁹

3.2. Fabrication of photopatterned ionogel microstructures.

Arrays of microstructures were photopolymerised by free radical polymerisation using the *in-house* designed photolithography set-up described in the Supportive Information. SEM images showed that the patterns were clear and well-defined (Figure 2) and demonstrate good compatibility of the ionogels with the photopatterning technique. Improved photolithographic microstructures were obtained by reducing the distance between the liquid pre-polymer and the mask to the thickness of the cover glass (170 μm). Further improvement could be achieved by decreasing the thickness of the glass slide, thus decreasing the distance between the pre-polymer and the mask.

It has been previously demonstrated that in the case of standard photo-curable materials, the dimensions of the resulting microstructures are sensitive to the UV exposure dose and the focal point of the light source.^{23,24} Our photolithography set-up takes advantage of these variables, and allows precise geometry control of the polymerised structures through control of the exposure time and the focal point of the light source (adjustable lens holder), thus users can easily define the dimensions and resolution of the structures according to their needs.

FIGURE 2

Figure 2. SEM pictures of the photo-responsive $[\text{P}_{6,6,6,14}][\text{NTf}_2]$ ionogel microstructures: rings (left) and lines (right), see Supporting Information Figure S3, for microstructure dimensions.

3.3. Characterisation of the swelling behaviour of the ionogel microstructures

The two main parameters used to characterise the swelling process of the ionogel microstructures are the degree of swelling, which corresponds to the relative change of the ionogel height (in our case %*H*) and the swelling time to reach the photostationary state.¹⁹ The 3D visualisation of the height change upon swelling of [P_{6,6,6,14}][dca] large disc ionogels is presented in Figure S4, Supporting Information. Each ionogel was analysed in triplicate and the resulting kinetic curves for the large disc-shaped ionogels are presented in Figure S5, Supporting Information. From the graphs it is evident that the swelling process is reproducible for each ionogel (see the Supporting Information, Figure S5) and microstructure (see the Supporting Information, Table S2). The average %*H* of the large disc microstructures during immersion in 1 mM HCl solution *versus* time is plotted in Figure 3a.

3.3.1. Swelling rates of the disc shaped phosphonium ionogels

First-order kinetic models were fitted (Microsoft Excel Solver)²² to the experimental data (Figure 3a) and the rate constants of the swelling process (k_{sw}) were estimated for each large disc-shaped ionogel using Eqn. 1. The swelling rate constant k_{sw} values obtained for all the ionogels fall into the same order of magnitude, Table 1. The value of k_{sw} for the [NTf₂]⁻ based ionogel ($5.3 \pm 0.1 \times 10^{-2} \text{ s}^{-1}$) is *ca.* 1.2 times larger than k_{sw} of [dca]⁻ ($4.5 \pm 0.3 \times 10^{-2} \text{ s}^{-1}$) and 1.4 times larger than k_{sw} of [Cl]⁻ ($3.9 \pm 0.2 \times 10^{-2} \text{ s}^{-1}$).

TABLE 1

When exposed to an acidic environment, non-polar, colourless “spiro” form (SP) spontaneously converts to the coloured “protonated merocyanine” form (MC-H⁺). The formation of MC-H⁺ leads to gel expansion in an acidic environment, however, for swelling to occur in the ionogels, the IL needs to be able to rearrange to accommodate not only water molecules but also the changing charged environment on the polymer (*i.e.* MC-H⁺). We suggest that the charge delocalisation of the IL anion may contribute significantly to the hydrogen ion transport during the protonation process of SP to MC-H⁺ and in turn to changing the ionogel environment from hydrophobic to more hydrophilic. The correlation between proton affinity and charge delocalisation of ionic liquid anions has been reported previously, whereby a greater degree of delocalisation lowers the proton affinity.²⁵ The swelling extent observed with these ionogels is in the order [NTf₂]⁻>[dca]⁻>Cl⁻, (in terms of the anion of the IL) which is the opposite that might be predicted on the basis of water uptake capacity of the pure ILs, which was reported previously as 0.7%, 3.1%, 8.0% w/w, respectively.²⁶ The reason for this difference in trend is not clear at this point, but it may lie in the way the ions interact with the gel polymer chains, and the impact of these interactions on IL nano-domain structure.^{27, 28}

In [P_{6,6,6,14}][Cl], the [Cl]⁻ anions are very closely associated with the [P_{6,6,6,14}]⁺ cations, to an extent wherein the charge is effectively shielded from the local environment, conveying a much more hydrophobic character to this ionic liquid than might be expected.²⁹ Consequently, the ionogels incorporating this IL do not swell to anything like the same extent as the gels incorporating [P_{6,6,6,14}][NTf₂], and [P_{6,6,6,14}][dca], as the ions in these latter ILs are less strongly associated, and therefore more free to exert their charged nature on their surrounding environment. Furthermore, in [dca]⁻, the negative charge is extensively delocalised from the

nitrogen across the whole molecule through π conjugation, reducing its impact compared to $[\text{NTf}_2]^-$.^{30, 31}

3.3.2. Percentage height change of ionogels upon swelling

The ionogels based on $[\text{P}_{6,6,6,14}][\text{dca}]$, $[\text{P}_{6,6,6,14}][\text{NTf}_2]$ and $[\text{P}_{6,6,6,14}][\text{Cl}]$ in the shape of large discs were kept in 1 mM HCl aqueous solution in the dark for 140 min at room temperature to study the time required to reach the photostationary state. All studied ionogels reached a steady-state swollen form after approximately 80 min and therefore, the shrinking behaviour was evaluated after soaking the ionogels microstructures in 1 mM HCl solution for 120 min, to be sure that they reached photostationary state, as explained before. As the ionogel is essentially anhydrous at the initial state, the chemical potential drive for water absorption into the IL is large, but despite this, there are significant differences in the degree of expansion between the phosphonium-based ionogels at the photostationary state. Values of %*H* for large disc ionogels microstructures at the photostationary state were $128 \pm 8\%$, $58 \pm 2\%$ and $20 \pm 3\%$ for $[\text{NTf}_2]^-$, $[\text{dca}]^-$ and $[\text{Cl}]^-$, respectively (Figure 3a). As shown in Figure 4 and Table S2, the same degree of swelling applies for all kinds of photopatterned microstructures. Depending on the shape of the microstructures, the %*H* of $[\text{P}_{6,6,6,14}][\text{NTf}_2]$, ionogels is in the range of 109 - 180%, followed by $[\text{P}_{6,6,6,14}][\text{dca}]$ ionogels (40 - 58%) and finally $[\text{P}_{6,6,6,14}][\text{Cl}]$ ionogels reaching just 20 - 27 %. Although $[\text{P}_{6,6,6,14}][\text{NTf}_2]$ is rather hydrophobic IL,²⁶ the $[\text{NTf}_2]^-$ anion can still re-arrange to accommodate a high amount of water within ionogel, thus resulting in

the largest increase in %H (Figure 3a and Figure 4). The %H order again follows increasing charge delocalisation from $[\text{Cl}]^- < [\text{dca}]^- < [\text{NTf}_2]^-$. The weakly basic $[\text{NTf}_2]^-$ anion exhibits an extensive charge delocalisation within the S-N-S backbone $[\text{NTf}_2]^-$ anion,³² and as a result it has a less affinity to nucleation sites in the p(SPNIpAAm) polymer backbone. As a consequence, the polar groups of the polymer and the $[\text{NTf}_2]^-$ anions are more free to interact with water, and $[\text{P}_{6,6,6,14}][\text{NTf}_2]$ ionogels therefore draw a higher amount of water into the polymer matrix, resulting in the fastest and largest %H. In contrast, the $[\text{Cl}]^-$ anion charge is highly localised, and interaction with the polymer backbone is much stronger.²⁹ Consequently, the $[\text{Cl}]^-$ anions and the polar groups on the polymer backbone are less free to interact with water molecules, and therefore the smallest percentage change in %H therefore occurs with $[\text{P}_{6,6,6,14}][\text{Cl}]$ based ionogels. The charge delocalisation of $[\text{dca}]^-$ anion is intermediate between the $[\text{NTf}_2]^-$ and $[\text{Cl}]^-$ anions used in this study, which is reflected in the intermediate extent of swelling observed with the corresponding $[\text{P}_{6,6,6,14}][\text{dca}]$ ionogel.

The trend in the degree of swelling in the ionogels may also be related to the contrasting cavities as the preparation IL was varied. SEM micrographs of the $[\text{P}_{6,6,6,14}][\text{NTf}_2]$, $[\text{P}_{6,6,6,14}][\text{dca}]$ and $[\text{P}_{6,6,6,14}][\text{Cl}]$ ionogel surfaces clearly show that the type of IL has significant influence on the morphology of the resulting material before and after hydration (see the Supporting Information, Figure S6). In its initial non-hydrated state, the $[\text{P}_{6,6,6,14}][\text{NTf}_2]$ ionogels display a structure with high cavities, efficiently pre-disposed for water uptake (see the Supporting Information, Figure S6a, left). As the hydration process proceeds, the morphology changes, clearly showing a fully saturated exterior (see the Supporting Information, Figure S6a, right).

Interestingly, under equivalent conditions $[P_{6,6,6,14}][dca]$ ionogel exhibits a more compact surface, whilst still smaller cavities in places (see the Supporting Information, Figure S6b). In contrast, the ionogel based on $[P_{6,6,6,14}][Cl]$ presented a distinctly different morphology in the non-hydrated and hydrated states, forming compact surface without any visible cavities (see the Supporting Information, Figure S6c). Solvatomorphological effects have been found to correlate with the %*H* values at the photostationary state – the more open matrix of the $[P_{6,6,6,14}][NTf_2]$ ionogel provides more surface area per unit volume to accommodate water (higher %*H*) in comparison to the $[P_{6,6,6,14}][dca]$ and $[P_{6,6,6,14}][Cl]$ ionogels, and this probably contributes to the more rapid kinetics of water uptake and release, and the greater extent of swelling (higher %*H*).

FIGURE 3

Figure 3. A) Swelling kinetics of pSPNIPAAm large disc ionogels in 1 mM HCl in the dark; and b) kinetics of shrinking induced by white light irradiation at 21 °C (n = 3).

FIGURE 4

Figure 4. Swelling (after 120 min; bright colours) and shrinking after 30 min (dark colours) %*H* values for all the ionogel microstructures when using $[P_{6,6,6,14}][Cl]$ (blue), $[P_{6,6,6,14}][dca]$ (green) and $[P_{6,6,6,14}][NTf_2]$ (red) (n = 3).

3.4. Influence of surface-area-to-volume ratio on the swelling rate of microstructures

The kinetics of swelling in ionogels is typically governed by diffusion-limited transport of the gel network in water,³³ and this is related to both the energy driving the process, and the surface area to volume ratio (SA/V). Therefore, miniaturisation of the gel features should yield an improvement in the rate of the swelling process¹⁹ since the rate of diffusion is inversely proportional to the square of the dimension of the gel.^{33, 34}

Therefore, the effect of SA/V of the microstructures on the swelling behaviour was investigated. Differently shaped [P_{6,6,6,14}][NTf₂] ionogels were photopolymerised as described before, and their SA/V values were estimated as follows: rings (SA/V = 0.0220 ± 0.0007), small discs (diameter = 250 μm , SA/V = 0.0150 ± 0.0003), large discs (diameter = 500 μm , SA/V = 0.0120 ± 0.0002) and lines (SA/V = 0.0090 ± 0.0006), as shown in Figure S3 (see the Supporting Information) and Figure 5. Each ionogel sample was immersed in 1 mM HCl aqueous solution in the dark at 21 °C and the %H value measured after 30 min. The results confirm that at a fixed time interval ($t = 30$ min) the higher the SA/V, the greater %H for all the ionogel microstructures tested. Figure 5 shows that the largest %H was observed for the rings, as these had the highest value of SA/V, while line shaped ionogels with the lowest SA/V ratio exhibited the smallest percentage of height change. The explanation for this behaviour lies in the swelling mechanism of the ionogel itself. If a structure is infinitesimally small (high SA/V ratio), then essentially everything is interfacial (surface) and there is no bulk. The swelling of such structures is described by a rate constant for interfacial transfer of water from the external solution into the interfacial polymer region, k_{int} . Therefore in the case of ionogel microstructures with high SA/V ratio values, *e.g.* rings, predominantly anisotropic water diffusion in the gel is very fast in all the gel matrix directions. Due to high surface-area-to-volume ratios at the microscale, mass

transfer times and diffusion distances are shorter, facilitating faster actuation times,³⁵ in our case - swelling.

However, once a bulk region is introduced (microstructures with small SA/V ratio values), two processes emerge:

1. Transfer of the water from the external solution into the interfacial region (this will have the same rate constant as above, k_{int}).
2. Diffusion of water from the interfacial region into the bulk (the rate constant will be different from (1) – slower (k_{bulk}); $k_{bulk} < k_{int}$).

With the increase of the bulk region, a whole series of bulk layers is envisaged with bulk-bulk water transfer rate constants, in which the transfer of water further into the bulk can only begin once water has reached the previous bulk layer. As a consequence, if the bulk region is made larger, the overall time for diffusion to establish a steady state throughout the entire structure becomes increasingly longer. Therefore, the effective rate constant for the structure changes with the bulk-to-surface ratio, but the fundamental processes involved are the same. This phenomenon clearly supports our findings, that the fastest water diffusion dependent swelling process occurs for ring-shaped ionogels, followed by small disc, large disc and line microstructures, see Figure 5.

FIGURE 5

Figure 5. %H after 30 min as a function of surface-area-to-volume ratio for the $[P_{6,6,6,14}][NTf_2]$ microstructures in the dark, immersed in 1 mM HCl; error bars are standard deviations, $n = 3$.

3.5. Characterisation of the shrinking behaviour of the ionogel microstructures

After immersion in HCl aqueous solution, the p(SPNIpAAm) ionogels have a yellowish color caused by the formation of the MC-H⁺ species. Exposure to white light induces photoisomerisation of the MC-H⁺ form to the closed spirobenzopyran chromophore SP, resulting in a change of the ionogel colour from yellow to white. The hydrophobic SP isomer induces the dehydration of the polymer and thus the shrinkage of the ionogel due to restructuring of the polymer matrix.

3.5.1. Shrinking rates of ionogel microstructures

The kinetics of the shrinking behaviour of [P_{6,6,6,14}][NTf₂], [P_{6,6,6,14}][dca] and [P_{6,6,6,14}][Cl] ionogels, monitored by white light irradiation for 30 min, shows that the IL plays an important role in the ionogel dehydration mechanism, similar to the swelling process. Figure S7, Supporting Information, presents the kinetic curves of the large disc ionogel microstructures analysed in triplicate, showing that the shrinking process is reproducible for each ionogel and the related microstructures (see the Supporting Information, Table S2). Under constant white light irradiation, the %H values vs. time were obtained, and the average values fitted to exponential models (Eqn. 2), see Figure 3b. Table 1 lists the shrinking rate constants of the ionogels. The largest shrinkage rate was observed for the [P_{6,6,6,14}][NTf₂] ionogel microstructures with $k_{sh} = 29 \pm 4 \times 10^{-2} \text{ s}^{-1}$, followed by [Cl]⁻ ($9 \pm 2 \times 10^{-2} \text{ s}^{-1}$) and [dca]⁻ ($8.3 \pm 0.9 \times 10^{-2} \text{ s}^{-1}$) based ionogels. A video of the [P_{6,6,6,14}][NTf₂] ring ionogel microstructures shrinking can be viewed at <http://tinyurl.com/d5yvq6l> (see the Supporting

Information, Figure S8).

Although stronger light irradiation may induce a faster isomerisation of the protonated merocyanine to spiropyran, the dehydration of the polymer and subsequent ionogel shrinkage is not an immediate process since it requires a few minutes to reach ca. 50% shrinkage of its initial swollen value. $[\text{NTf}_2]^-$ ionogels reached 50% of their swollen height after 3 min, $[\text{Cl}]^-$ after 10 min and $[\text{dca}]^-$ after 15 min of irradiation, Figure 3b. However, it is important to mention that when these materials are incorporated within micro-fluidic manifolds for microvalve applications, only a relatively small percentage of height change is required to open the valve. Therefore, valves based on these materials in micro-fluidic channels will typically occur at much shorter timescales (seconds).¹⁸

The %*H* of all the photopolymerised microstructures was measured after 30 min (Figure 3b, Figure 4) of white light irradiation following the same protocol described above. In all cases, the $[\text{P}_{6,6,6,14}][\text{NTf}_2]$ microstructures exhibit the greatest %*H* reduction, followed by $[\text{P}_{6,6,6,14}][\text{dca}]$ and $[\text{P}_{6,6,6,14}][\text{Cl}]$. There are several interesting outcomes arising from these experiments. For all the ionogels, the water release is clearly dependent on the IL encapsulated in the crosslinked p(SPNIpAAm) ionogel. As the ionogel shrinks, the water and ionic liquid interactions with the polymer backbone (eg. hydrogen bonding with pNIPAAm amide groups) are reduced in favour of increasingly strong polymer-polymer hydrogen bonding. In turn, the gel adopts more compact format, which also reduces the free volume available for water to occupy. This effect is more apparent in ionogels with more hydrophobic ionic liquids, such as $[\text{P}_{6,6,6,14}][\text{NTf}_2]$, leading to greater and faster shrinkage. Our experiments demonstrate that the ionogel k_{sh} increases with increasing hydrophobicity of the IL. Dehydration is more favourable for $[\text{NTf}_2]^-$ than for $[\text{Cl}]^-$ and $[\text{dca}]^-$, since

[NTf₂]⁻ presents six hydrophobic fluoride groups and consequently, exhibits larger tendency towards dehydration.²⁶ The water release process is triggered by MC-H⁺ – SP conversion, during which the polarity of the ionogel changes from hydrophilic to hydrophobic.²⁹ Therefore, the induced water expulsion will be promoted by more hydrophobic ILs, such as [P_{6,6,6,14}][NTf₂], resulting in faster shrinking in comparison to more hydrophilic ionogels using ILs such as [P_{6,6,6,14}][dca] or [P_{6,6,6,14}][Cl]. The [NTf₂]⁻ based ionogel shows the fastest shrinking of the three ionogels, in agreement with previous published work,³⁶ that explains how [NTf₂]⁻ anion does not interact with the MC form and therefore it does not inhibit the light induced thermal relaxation of MC to its ground non-zwitterionic state.

Another factor that can attribute to the shrinkage rates are the cavities of the ionogel structure, as this affects the SA/V ratio, and provides effective routes for water transport into and out of the bulk gel structure.⁹ This is consistent with the behaviour of the [NTf₂]⁻ ionogels compared to the other ionogels, as it exhibits a structure with cavities (see the Supporting Information, Figure S6) and has the fastest shrinking kinetics. The most probable reason for the rapid shrinking of the ionogels is the presence of large cavities, and the open network mesh structure, which allows rapid collapse of the polymer chains.³⁷

3.5.2. Height change of ionogels upon shrinking process

Figure 3b and Figure 6 show that after 30 min of white light irradiation, each ionogel microstructure exhibited various degrees of expulsion of absorbed water. [NTf₂]⁻ disc ionogels exhibit a total of 108% shrinkage, reaching *ca.* 15% of the

ionogel height in its swollen state (H_{sw}). In the case of $[dca]^-$ based microstructures, they exhibit 42% shrinkage reaching also *ca.* 15% of their H_{sw} for the same irradiation time. Finally, $[Cl]^-$ ionogels exhibit the smallest percentage shrinking (16%). However, after 30 min of irradiation they reached 4% of H_{sw} , indicating that they almost reverted back to their initial size, prior to swelling.

FIGURE 6

Figure 6. Ionogel small discs: (a) $[P_{6,6,6,14}][NTf_2]$, (b) $[P_{6,6,6,14}][dca]$ and (c) $[P_{6,6,6,14}][Cl]$ after photopolymerisation (left); swelling in 1 mM HCl solution for 2 h (middle) and shrinking upon white light irradiation (right).

These experimental results demonstrate that the swelling and shrinking behaviour of the ionogels are strongly influenced by the ionic liquid incorporated into the gel during photopolymerisation. Dramatic differences in swelling/shrinking behaviour of the ionogels can be seen if the ionic liquid is used alone or in a mixture with other organic solvents. In previous work, the order of swelling and shrinking behaviour found with similar ionogels produced using 1:1 butanol IL v/v was different ($[P_{6,6,6,14}][dca]$ based ionogels were faster than ionogels incorporating $[P_{6,6,6,14}][NTf_2]$). The reason for this difference is not clear at present, but may lie in differing amounts of residual butanol remaining in the ionogels after formation, which affects the overall gel polarity and affinity for water. This opens the possibility of tuning the behaviour of the microvalves by varying the solvent composition used for the synthesis of ionogel.

4. Conclusions

A variety of phosphonium based ionogel microstructures were fabricated, including discs, rings and lines, and their volume phase transition behaviour and swelling/shrinkage kinetics were investigated. Results show that the ionic liquids entrapped within the polymer matrix have a significant influence on the swelling and shrinking of the ionogel microstructures. It was found that the p(SPNIpAm) swelling/shrinking properties could be significantly altered by varying the anion of the phosphonium IL. [P_{6,6,6,14}][NTf₂] ionogel microstructures undergo the largest volume expansion, up to 180% of their initial size, and the fastest swelling and shrinking kinetics ($k_{sw} = 5.3 \pm 0.1 \times 10^{-2} \text{ s}^{-1}$ and $k_{sh} = 29 \pm 4 \times 10^{-2} \text{ s}^{-1}$). It has been proved that each ionic liquid provides a specific and well defined degree of volume change (%*H*) and photoresponse time of the microstructures. Therefore, this work presents the tremendous potential of using ionogels microstructures as microactuators with potential in micro-fluidic applications and set the basis for our ongoing work to develop photoswitchable ionogel microvalves within micro-fluidic manifolds.

ASSOCIATED CONTENT

Supporting Information

Photolithography set-up and photomasks used for fabrication of ionogel microstructures, contact angle results, details of ionogel microstructures, SEM of ionogels, experimental kinetics curves of ionogel swelling and shrinking, images of ionogel microstructures after swelling and shrinking.

Acknowledgements

M.C wishes to thank to the Marie Curie Initial Training Network funded by the EC

FP7 People Program ATWARM (Advanced Technologies for Water Resource Management, Marie Curie ITN, No. 238273). K.J.F thanks Marie Curie Actions re-integration grant PIRG07-GA-2010-268365. D.D & F.B.L thank the Science Foundation Ireland under grant 07/CE/I1147. The authors are grateful to Dr. Al Robertson from Cytec® industries for the generous donation of phosphonium ILs. The authors would also like to thank Dr. Katya Izgorodina, Monash University, for useful discussion throughout and Larisa Florea for assistance in taking SEM micrographs.

References

- (1) Czugała, M.; Ziolkowski, B.; Byrne, R.; Diamond, D.; Benito-Lopez, F., Materials science: the key to revolutionary breakthroughs in micro-fluidic devices. *Proc. SPIE 8107, Nano-Opto-Mechanical Systems (NOMS) 2011*, 81070C-81070C.
- (2) Xie, Z.-L.; Jelacic, A.; Wang, F.-P.; Rabu, P.; Friedrich, A.; Beuermann, S.; Taubert, A., Transparent, flexible, and paramagnetic ionogels based on PMMA and the iron-based ionic liquid 1-butyl-3-methylimidazolium tetrachloroferrate(iii) [Bmim][FeCl₄]. *Journal of Materials Chemistry 2010*, 20 (42), 9543-9549.
- (3) Suzuki, H., Stimulus-responsive Gels: Promising Materials for the Construction of Micro Actuators and Sensors. *Journal of Intelligent Material Systems and Structures 2006*, 17 (12), 1091-1097.
- (4) Lo, C.-W.; Zhu, D.; Jiang, H., An infrared-light responsive graphene-oxide incorporated poly(N-isopropylacrylamide) hydrogel nanocomposite. *Soft Matter 2011*, 7 (12), 5604.
- (5) Orlov, M.; Tokarev, I.; Scholl, A.; Doran, A.; Minko, S., pH-Responsive Thin Film Membranes from Poly(2-vinylpyridine): A Water Vapor-Induced Formation of a Microporous Structure. *Macromolecules 2007*, 40 (6), 2086-2091.
- (6) Liu, F.; Urban, M. W., Challenges and Opportunities in Stimuli-Responsive Polymeric Materials. *Prog. Polym Sci 2010*, 35 (3).
- (7) Inomata, H.; Goto, S.; Saito, S., Phase transition of N-substituted acrylamide gels. *Macromolecules 1990*, 23 (22), 4887-4888.
- (8) Ziolkowski, B.; Czugała, M.; Diamond, D., Integrating stimulus responsive materials and microfluidics: The key to next-generation chemical sensors. *Journal of Intelligent Material Systems and Structures 2012*.
- (9) Wu, X. S.; Hoffman, A. S.; Yager, P., Synthesis and characterization of thermally reversible macroporous poly(N-isopropylacrylamide) hydrogels. *Journal of Polymer Science Part A: Polymer Chemistry 1992*, 30 (10), 2121-2129.
- (10) Sugiura, S.; Sumaru, K.; Ohi, K.; Hiroki, K.; Takagi, T.; Kanamori, T., Photoresponsive polymer gel microvalves controlled by local light irradiation. *Sensors and Actuators A: Physical 2007*, 140 (2), 176-184.
- (11) Satoh, T.; Sumaru, K.; Takagi, T.; Kanamori, T., Fast-reversible light-driven hydrogels consisting of spirobenzopyran-functionalized poly(N-isopropylacrylamide). *Soft Matter 2011*, 7 (18), 8030-8034.

- (12) Sumaru, K.; Ohi, K.; Takagi, T.; Kanamori, T.; Shinbo, T., Photoresponsive Properties of Poly(N-isopropylacrylamide) Hydrogel Partly Modified with Spirobenzopyran. *Langmuir* **2006**, *22* (9), 4353-4356.
- (13) Sugiura, S.; Szilagy, A.; Sumaru, K.; Hattori, K.; Takagi, T.; Filipcsei, G.; Zrinyi, M.; Kanamori, T., On-demand microfluidic control by micropatterned light irradiation of a photoresponsive hydrogel sheet. *Lab on a Chip* **2009**, *9* (2), 196-198.
- (14) Kavanagh, A.; Byrne, R.; Diamond, D.; Fraser, K. J., Stimuli Responsive Ionogels for Sensing Applications—An Overview. *Membranes* **2012**, *2* (1), 16-39.
- (15) Gallagher, S.; Kavanagh, A.; Florea, L.; MacFarlane, D. R.; Fraser, K. J.; Diamond, D., Temperature and pH triggered release characteristics of water/fluorescein from 1-ethyl-3-methylimidazolium ethylsulfate based ionogels. *Chemical Communications* **2013**, *49* (41), 4613-4615.
- (16) F. Benito-Lopez; S. Coyle; R. Byrne; M. O'Toole; C. Barry; D. Diamond, Simple barcode system based on ionogels for real time pH-sweat monitoring. In *BSN 2010 - 7th International Workshop on Wearable and Implantable Body Sensor Network*, Singapore, 2010; pp 291-296.
- (17) Kavanagh, A.; Byrne, R.; Diamond, D.; Radu, A., A two-component polymeric optode membrane based on a multifunctional ionic liquid. *Analyst* **2011**, *136* (2), 348-353.
- (18) Benito-Lopez, F.; Byrne, R.; Răduță, A. M.; Vrana, N. E.; McGuinness, G.; Diamond, D., Ionogel-based light-actuated valves for controlling liquid flow in microfluidic manifolds. *Lab on a Chip* **2010**, *10* (2), 195-201.
- (19) Mateescu, A.; Wang, Y.; Dostalek, J.; Jonas, U., Thin Hydrogel Films for Optical Biosensor Applications. *Membranes* **2012**, *2* (1), 40-69.
- (20) A. Szilagy, K. S., S. Sugiura, T. Takagi, T. Shinbo, M. Zrinyi, T. Kanamori, Rewritable microrelief formation on photoresponsive hydrogel layers. *Chem. Mater.* **2007**, *19*, 2730-2732.
- (21) C. Hou, A. E. H., Ultrashort separation length homogeneous electrophoretic immunoassays using on-chip discontinuous polyacrylamide gels. *Analytical Chemistry* **2010**, *82* (8), 3343-51.
- (22) Diamond, D.; Hanratty, V. C. A., *Spreadsheet Applications for Chemistry Using Microsoft Excel*. John Wiley and Sons: New York, 1997.
- (23) Kavanagh, A.; Copperwhite, R.; Oubaha, M.; Owens, J.; McDonagh, C.; Diamond, D.; Byrne, R., Photo-patternable hybrid ionogels for electrochromic applications. *Journal of Materials Chemistry* **2011**, *21*, 8687-8693.
- (24) Narayan, R. J.; Doraiswamy, A.; Chrisey, D. B.; Chichkov, B. N., Medical prototyping using two photon polymerization. *Materials Today* **2010**, *13* (12), 42-48.
- (25) Izgorodina, E. I.; Forsyth, M.; MacFarlane, D. R., Towards a Better Understanding of Delocalized Charge in Ionic Liquid Anions. *Australian Journal of Chemistry* **2007**, *60* (1), 15-20.
- (26) Forsyth, S. A.; Pringle, J. M.; MacFarlane, D. R., Ionic Liquids - An Overview. *Australian Journal of Chemistry* **2004**, *57* (2), 113-119.
- (27) Shimizu, K.; PaÅÅdua, A. A. H.; Canongia Lopes, J. N., Nanostructure of Trialkylmethylammonium Bistriflamide Ionic Liquids Studied by Molecular Dynamics. *The Journal of Physical Chemistry B* **2010**, *114* (47), 15635-15641.
- (28) Coleman, S.; Byrne, R.; Minkovska, S.; Diamond, D., Investigating Nanostructuring within Imidazolium Ionic Liquids: A Thermodynamic Study Using Photochromic Molecular Probes. *The Journal of Physical Chemistry B* **2009**, *113* (47), 15589-15596.

- (29) Thompson, D.; Coleman, S.; Diamond, D.; Byrne, R., Electronic structure calculations and physicochemical experiments quantify the competitive liquid ion association and probe stabilisation effects for nitrobenzospiropyran in phosphonium-based ionic liquids. *Physical Chemistry Chemical Physics* **2011**, *13* (13), 6156-6168.
- (30) Deng, M.-J.; Chen, P.-Y.; Leong, T.-I.; Sun, I. W.; Chang, J.-K.; Tsai, W.-T., Dicyanamide anion based ionic liquids for electrodeposition of metals. *Electrochemistry Communications* **2008**, *10* (2), 213-216.
- (31) Illner, P.; Begel, S.; Kern, S.; Puchta, R.; van Eldik, R., Fast Substitution Reactions of Pt(II) in Different Ionic Liquids. Reactivity Control by Anionic Components, \ddagger . *Inorganic Chemistry* **2008**, *48* (2), 588-597.
- (32) Forsyth, C. M.; MacFarlane, D. R.; Golding, J. J.; Huang, J.; Sun, J.; Forsyth, M., Structural Characterization of Novel Ionic Materials Incorporating the Bis(trifluoromethanesulfonyl)amide Anion. *Chemistry of Materials* **2002**, *14* (5), 2103-2108.
- (33) Yoshida, R.; Uchida, K.; Kaneko, Y.; Sakai, K.; Kikuchi, A.; Sakurai, Y.; Okano, T., Comb-type grafted hydrogels with rapid deswelling response to temperature changes. *Nature* **1995**, *374* (6519), 240-242.
- (34) Tanaka, T.; Sato, E.; Hirokawa, Y.; Hirotsu, S.; Peetermans, J., Critical Kinetics of Volume Phase Transition of Gels. *Physical Review Letters* **1985**, *55* (22), 2455-2458.
- (35) Teh, S.-Y.; Lin, R.; Hung, L.-H.; Lee, A. P., Droplet microfluidics. *Lab on a Chip* **2008**, *8* (2), 198-220.
- (36) Byrne, R.; Fraser, K. J.; Izgorodina, E.; MacFarlane, D. R.; Forsyth, M.; Diamond, D., Photo- and solvatochromic properties of nitrobenzospiropyran in ionic liquids containing the [NTf₂]⁻ anion. *Physical Chemistry Chemical Physics* **2008**, *10* (38), 5919-5924.
- (37) Li, X.; Wu, W.; Liu, W., Synthesis and properties of thermo-responsive guar gum/poly(N-isopropylacrylamide) interpenetrating polymer network hydrogels. *Carbohydrate Polymers* **2008**, *71* (3), 394-402.

BIOGRAPHIES:

Monika Czugala received her MSc. Eng. Degree from West Pomeranian University of Technology in Szczecin, Poland, in Materials Engineering in 2010. In 2010 she joined the Adaptive Sensors Group of Prof. Dermot Diamond to start Ph.D. as a fellow of the Marie Curie Initial Training Network ATWARM program. She finished her Ph.D. in 2013.

Candice Blin received her M.S. degree in 2011 in nanotechnology from the Graduate School of Chemistry and Physics of Bordeaux, France. She began her PhD thesis on diamond photonic crystals for biosensing applications at the Diamond Sensors Laboratory of the French Atomic Energy Center (CEA LIST), in tight collaboration with the Institute of Fundamental Electronics of University Paris Sud 11, France. Her research interests are concerned with microfabrication on diamond, photonics, optical sensors and biochemical sensors.

Peer Fischer is a Professor of Physical Chemistry at the University of Stuttgart and he heads the Micro Nano and Molecular Systems Lab at the Max Planck Institute for Intelligent Systems in Stuttgart. He received a BSc. degree in Physics from Imperial College London and a Ph.D. from the University of Cambridge. He was a visiting

scientist at the European Laboratory for Nonlinear Spectroscopy in Florence (LENS) and a NATO Postdoctoral Fellow at Cornell University, before joining the Rowland Institute at Harvard. At Harvard he held a Rowland Junior Research Fellowship and directed an interdisciplinary research lab for five years. In 2011 he moved his lab to the Max-Planck-Institute for Intelligent Systems in Stuttgart, where he is an independent, tenured PI.

Kevin J. Fraser received his M.Sc. in 2004 from the University of Aberdeen, Scotland. He completed his Ph.D. under the supervision of Professor D. R. MacFarlane entitled 'Physical Properties of Phosphonium Based Ionic Liquids' at Monash University, Melbourne in 2008. Currently he is a Marie Curie Postdoc working with Prof Dermot Diamond at the National Centre for Sensor Research (www.ncsr.ie), Dublin City University, Ireland. Kevin is a qualified physical chemist & materials engineer with over 8 years experience in the field. He is an academic referee for Elsevier, Royal Society of Chemistry and the American Chemical Society. He is author on 28 international peer reviewed journals (3 cover articles, H-index 11) and 1 patent protecting his work.

Fernando Benito López studied chemistry at the Universidad Autonoma de Madrid and completed his master studies in the Department of Inorganic Chemistry in 2002. He obtained his PhD at the University of Twente, The Netherlands, under the supervision of Prof. David N. Reinhoudt in 2007. He carried out his postdoctoral research in the group of Prof. Dermot Diamond at Dublin City University, Dublin, Ireland. From 2010, he is Team Leader in polymer microfluidics at CLARITY:

Centre for Sensor Web Technology, National Centre for Sensor Research, Dublin City University. From 2012 he is Senior Scientist at CIC microGUNE, Spain.

Dermot Diamond received his PhD and DSc from Queen's University Belfast (Chemical Sensors, 1987, Internet Scale Sensing, 2002), and was VP for Research at Dublin City University (2002–2004). He has published over 200 peer-reviewed papers in international journals, is a named inventor in 13 patents, and is co-author and editor of three books. He is currently director of the National Centre for Sensor Research (www.ncsr.ie) and SFI INSIGHT Investigator, (<http://www.insight-centre.org/>), a major research initiative focused on wireless sensor networks. In 2002 he was awarded the inaugural silver medal for Sensor Research by the RSC, London.

Table 1. Rate constants of swelling and shrinking of pSPNIPAAm ionogels at 21 °C (n = 3).

IL used	Average k_{sw}	Average k_{sh}
[P _{6,6,6,14}][NTf ₂]	5.3 ± 0.1	29 ± 4
[P _{6,6,6,14}][dca]	4.5 ± 0.3	8.3 ± 0.9
[P _{6,6,6,14}][Cl]	3.9 ± 0.2	9 ± 2

Table S1. Contact angle values of the functionalised glass slide surfaces (n = 4).

Metho d No.	After cleaning [°]	I NaOH [°]	III MPTMS [°]
1	61 ± 3	52 ± 1	72 ± 4

Table S2. Percentage change height (%H) of the ionogel microstructures during the swelling and shrinking process (n = 3).

IL used for ionogel synthesis	Small discs		Large discs		Rings		Lines	
	Swelli ng [%]	Shrinki ng [%]	Swelli ng [%]	Shrinki ng [%]	Swelli ng [%]	Shrinki ng [%]	Swelli ng [%]	Shrinki ng [%]
[P _{6,6,6,14}][N Tf ₂]	140 ± 6	122 ± 11	123 ± 2	108 ± 3	180 ± 8	166 ± 14	109 ± 5	91 ± 7
[P _{6,6,6,14}][dc a]	56 ± 8	42 ± 2	58 ± 2	42 ± 2	56 ± 6	44 ± 3	40 ± 1	35 ± 7
[P _{6,6,6,14}][Cl]	23 ± 5	18 ± 3	20 ± 5	16 ± 2	26 ± 8	16 ± 3	24 ± 1	17 ± 3

Highlights

Micropatterned photoresponsive ionogel microstructures using phosphonium ionic liquids.

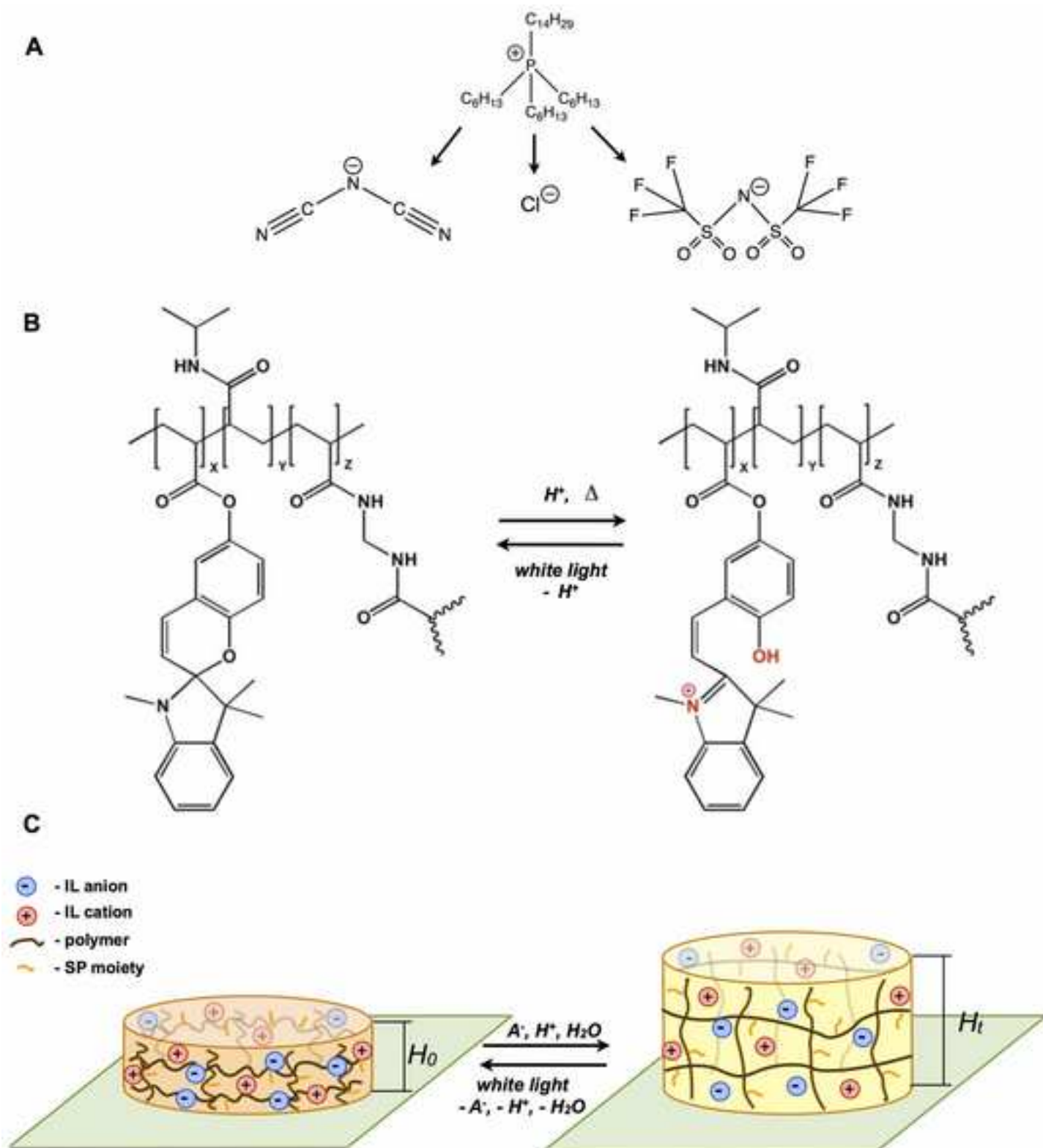
Stimuli responsive materials actuated using light irradiation.

Characterisation of the swelling and shrinking behaviour of the ionogel microstructures.

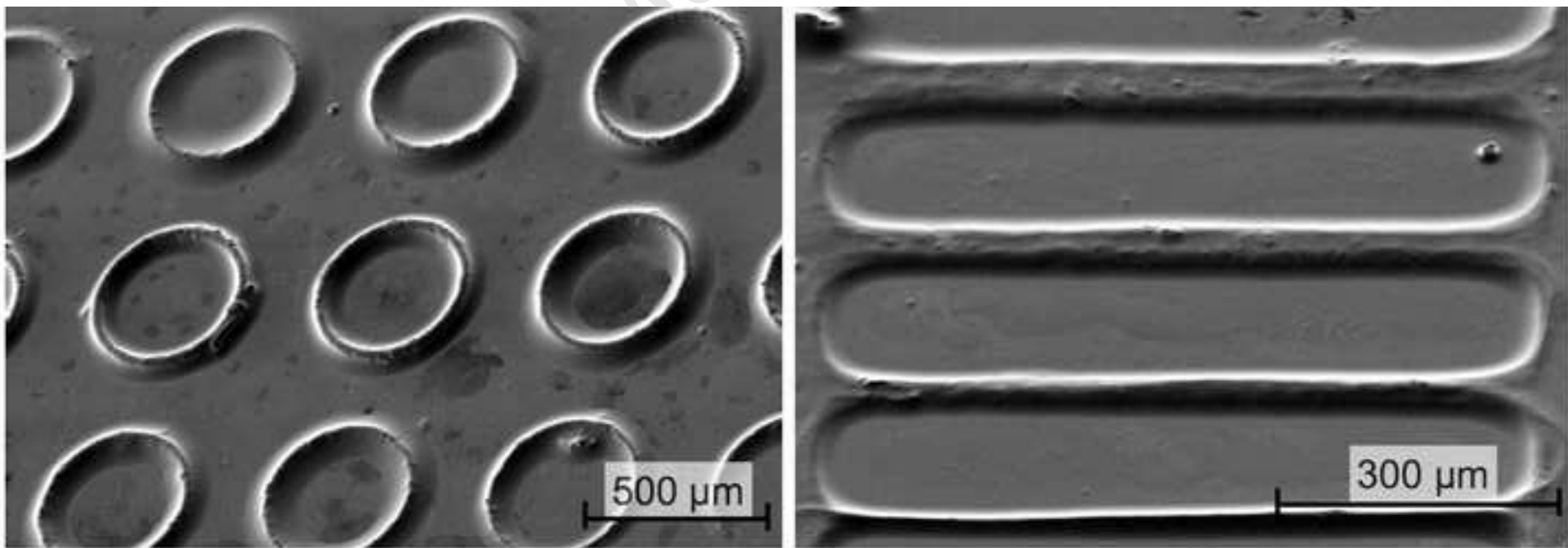
Influence of surface-area-to-volume ratio on the swelling/shrinking kinetics.

[P_{6,6,6,14}][NTf₂] ionogel exhibits the greatest swelling 180% and the fastest shrinkage rate.

Accepted Manuscript



Manuscript



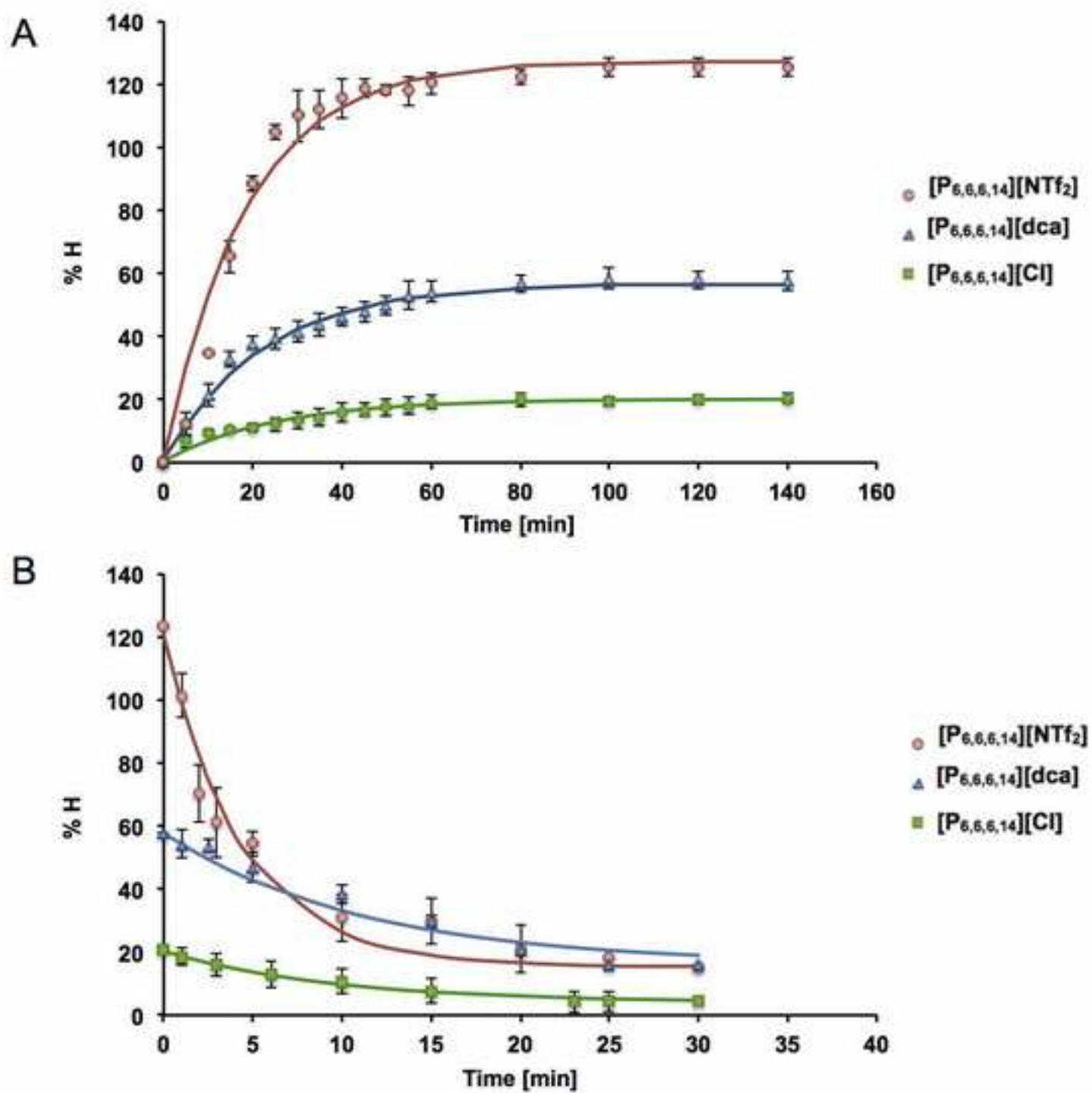


Figure4

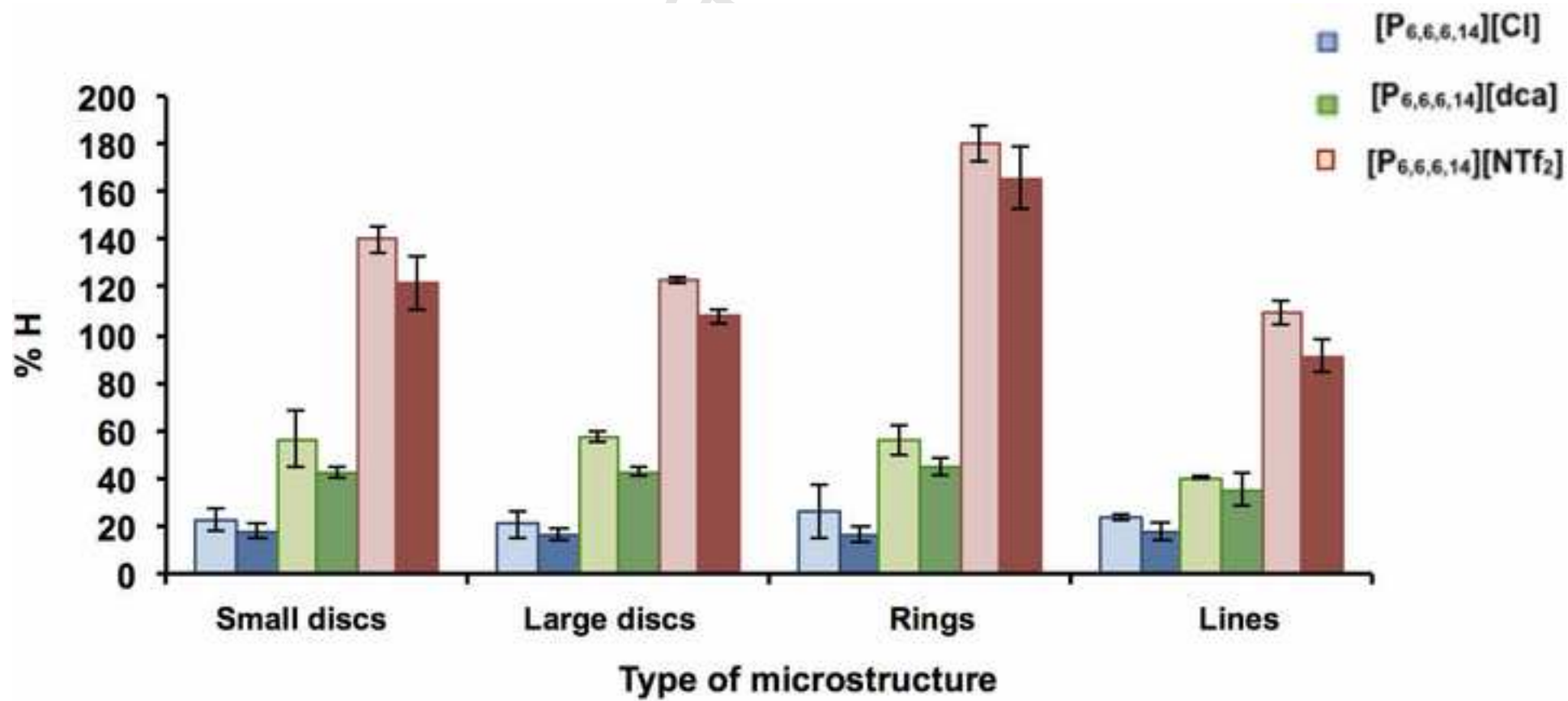
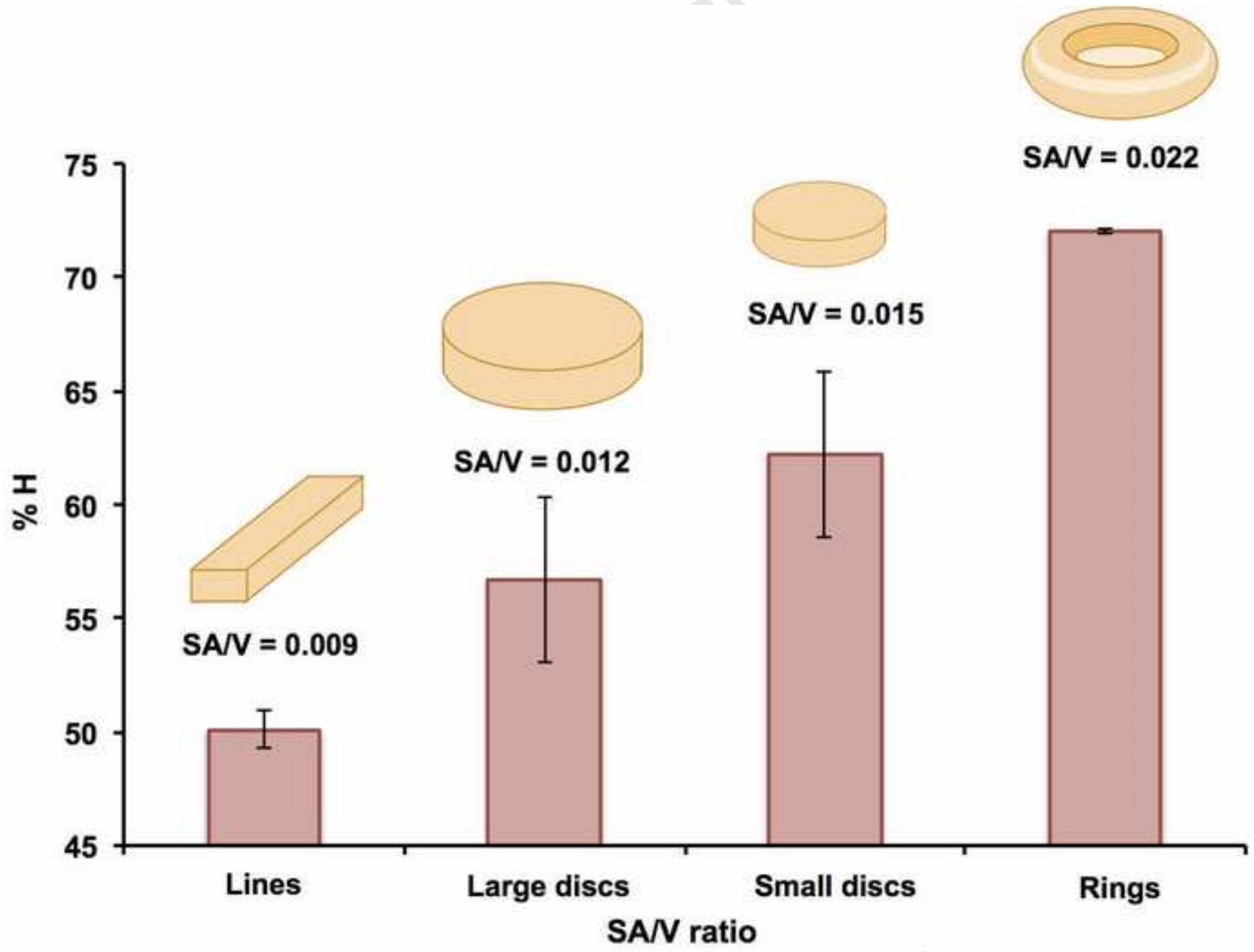
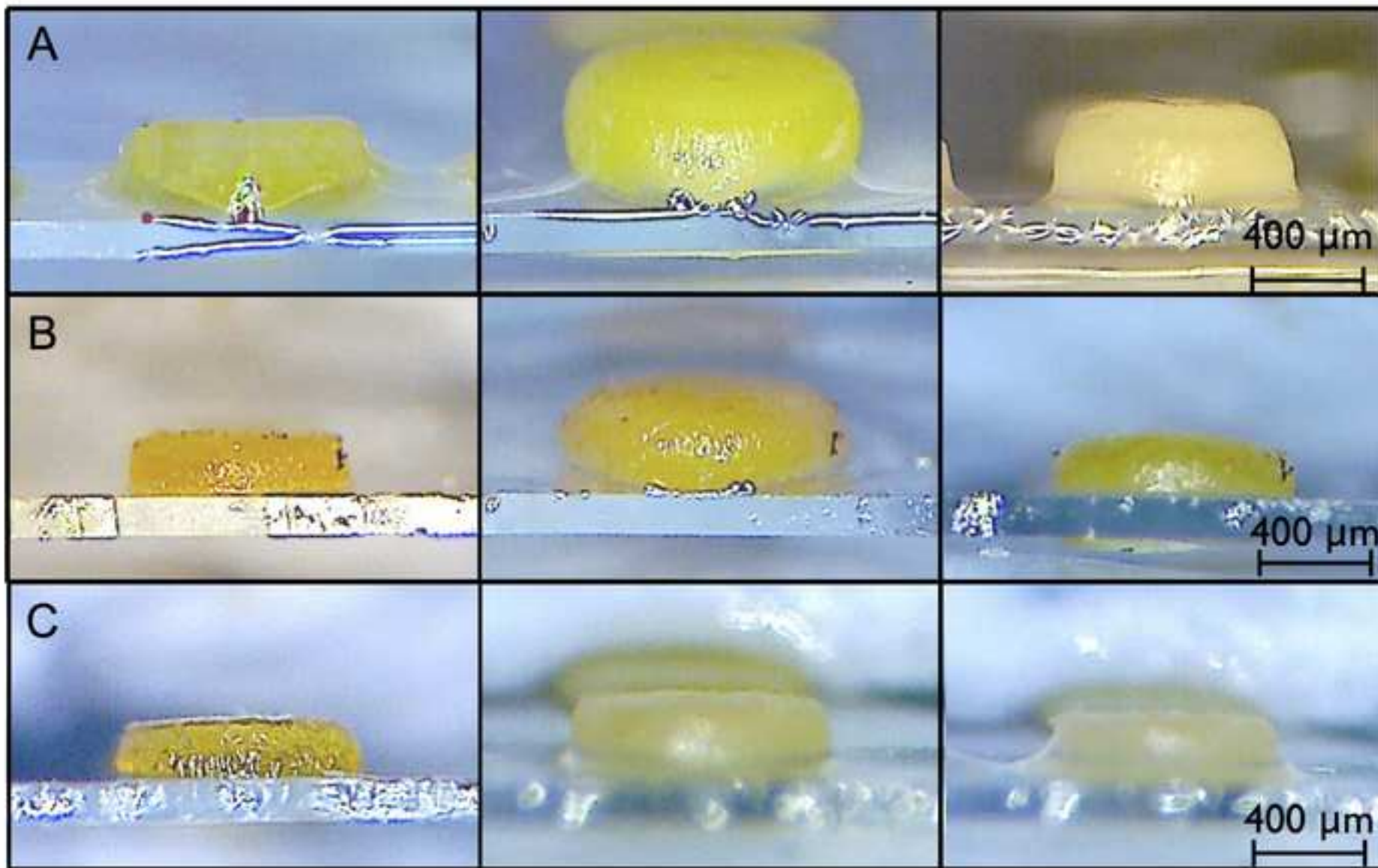


Figure 5

trip



scrip



Manuscript

